Finite Element for Flow Problems (Papers)
FEF05 IACM Special Interest Conference supported by ECCOMAS, April 4-6, 2005, Swansea, Wales, UK

On Level Set modelling of Bi-fluid capillary flow

Anne-Cécile Lesage[1,2*], Olivier Allain[1], Alain Dervieux[2,1]

[1] LEMMA, 938-A, avenue de la république, 06550 La Roquette-sur-Siagne, France
[2] INRIA, BP 93, 2004 route des Lucioles, 06902 Sophia-Antipolis, France
contact: alain.dervieux@inria.fr

SUMMARY

We consider the adaptation of a level set method for the simulation of capillary flows on unstructured meshes. The advection step is first analysed. In order not to loose accuracy, this step should be one order more accurate that the discretisation of velocity. We then compare different ways in choosing the level set velocity and in re-initialising the level set function between advection phases without loosing too much accuracy. Applications to Rayleigh flows and to reorientation with contact angle are presented.

KEY WORDS: incompressible Navier-Stokes; finite element method; interface tracking; capillarity; contact angle

1 Introduction

Interface motion simulation has been studied from the early start of computer simulation. The Level Set (LS) principle introduced in the late 80's by Osher and Sethian proposes to advect a relatively smooth field ϕ the zero contour of which is the interface to represent. Since the function to advect is smooth, this method opens the door to an accuracy higher than first-order. It combines also well to a finite-element discretization, the intrinsic interpolation of which specifies accurately the interface location.
Also, the combination of level set and finite element lends itself to an easy discretisation on unstructured meshes. However, cartesian discretisations may enjoy convergence of dependant variables *and* of their derivatives. In contrast, for unstructured meshes, surfaces traces and derivatives may have much poorer convergence, if any. Then, in order to obtain for the global scheme an order of accuracy better than unity, several numerical mechanisms have to be carefully combined with the initial simple idea:
- Function ϕ should be advected with sufficient accuracy.
- Function ϕ should be maintained sufficiently smooth, and of not too small gradient near its zero contour, this for an accurate motion, an accurate location of the interface, and an accurate evaluation of its curvature. This will be the role of a re-initisalisation step.
- Contact angle modelling also require particular attention in order to avoid a too unsmooth level set volumic field and velocity.

Next section recalls the main features of LS method. In Sec.3, by analysing the advection step, we give a lower estimate of the accuracy of the method under gradient conditions. Section 4 examines some means for satisfying gradient conditions without introducing new error sources. We propose a family of formulation which permits to take into account accurately the local orientation of a solid wall. Sections 5 and 6 are devoted to the experimentation of the proposed options for capillary flows without and with contact angle.

2 Main features of the Level Set Method

Let us consider the following model for the flow of two incompressible immiscible fluids with interface tension:

$$\begin{aligned} \rho\frac{\partial \mathbf{U}}{\partial t} \; + \; \rho\nabla.(\mathbf{U}\otimes\mathbf{U}) \; - \; \nabla.(2\mu(\rho)\mathbf{D}) \; + \; \nabla p \; + \; \sigma\kappa(\rho)\delta(\rho)\mathbf{n} \; - \; \rho\mathbf{g} \; = \; 0 \\ \partial_t\rho + \nabla.(\rho\mathbf{U}) = 0 \qquad \rho = \rho_l \; or \; \rho_g \\ \nabla.\mathbf{U} = 0 \end{aligned} \tag{1}$$

In this formulation , the fluid velocity is denoted $\mathbf{U}$, and the pressure p. The density ρ takes only two values in two subdomains separated by an interface smooth enough for allowing to consider its normal:

$$\mathbf{n}\delta(\rho) \; = \; \frac{1}{\rho_l - \rho_g}\nabla\rho \; , \tag{2}$$

further, $\delta(\rho)$ denotes the Dirac delta function on the interface, σ the surface tension coefficient, $\kappa(\rho)$ the curvature of the interface, $\mathbf{g}$ the gravity volumic force, $\mathbf{D} = \frac{1}{2}(\nabla\mathbf{U} + \nabla(\mathbf{U})^T)$ the deformation tensor, $\mu(\rho)$ the dynamic viscosity and ρ_l, ρ_g the two values taken by the density in each fluid. Typically ρ_l in the liquid and ρ_g in the gas.

In the case where $\sigma = 0$ and $\mu(\rho)$ is a constant, this model is a particular case of the heterogeneous Navier-Stokes model as analysed in [2] and [3] . The discontinuity in the density is the cause of difficulties in the approximation of the advection of the interface Γ separing the two components of different density, in conservation of moments, and in imposing incompressibility. In this paper we concentrate on the interface advection. It can be written with the characteristic function χ of liquid phase

$$\frac{\partial \chi}{\partial t} \; + \; \mathbf{U}\cdot\nabla\,\chi \; = \; 0 \quad (\chi = 0 \; or \; 1).$$

The characteristic function can be used to define the density distribution.

$$\rho \; = \; \chi\rho_l \; + \; (1-\chi)\rho_g.$$

The formal accuracy of the advection of a step function as χ is severely limited to first order unless the numerical scheme cleverly exploits the fact that χ takes only two different values. A particular way of doing this is the second-order VOF method (see for example [1]) which we do not discuss further here.

Let H be the step function such that $H(x) = 1$ if $x > 0$ and $H(x) = 0$ elsewhere. The Level Set method introduced by Osher et Sethian ([6]) relies on smoother function ϕ such that $\chi = H(\phi)$ where $H(\phi)$ is the Heavyside function on the interface Γ:

$$\frac{\partial \phi}{\partial t} \; + \; \mathbf{U}\cdot\nabla\,\phi \; = \; 0 \; ; \; \chi = H(\phi) \tag{3}$$

ϕ is initialised and periodically reset as the signed-distance to the interface $\phi \; = \; \pm \; d(\Gamma)$ ([7],[8]). We take $\phi \; < \; 0$ in the gas region and $\phi \; > \; 0$ in the liquid region. The interface is the zero level set of ϕ.

$$\Gamma \; = \; \{\mathbf{x} \mid \phi(\mathbf{x},t) = 0\} \tag{4}$$

We take $\phi \; < \; 0$ in the gas region and $\phi \; > \; 0$ in the liquid region. Using the ϕ function, the previous governing equation for the fluid velocity $\mathbf{U}$ and the pressure p along with boundary conditions can be written as a single equation with a Continuous Surface Force ([5]) formulation of the surface tension term ([9]),

$$\rho(\phi)\frac{D\mathbf{U}}{Dt} \; = \; -\nabla p + \nabla.(2\mu(\phi)\mathbf{D}) - \sigma\kappa(\phi)\delta(\phi)\nabla(\phi) + \rho(\phi)\mathbf{g} \; . \tag{5}$$

The surface tension force is modelled as a volumic interfacial force on a thickened interface. $\kappa(\phi)$ is the curvature computed in all the domain as the second derivative of ϕ.

$$\kappa(\phi) \;=\; \nabla.(\mathbf{n}) \;=\; \nabla.(\frac{\nabla\phi}{|\nabla\phi|}) \tag{6}$$

The density and the viscosity are constant in each fluid, we can write

$$\begin{aligned}\rho(\phi) \;&=\; \rho_g \;+\; (\rho_g \;-\rho_l)\; H(\phi)\\ \mu(\phi) \;&=\; \mu_g \;+\; (\mu_g \;-\mu_l)\; H(\phi).\end{aligned}$$

The most usual level set method can be defined rather accurately according to the following stages:

Stage 1: define an advection velocity for the level set,

Stage 2: advect the ϕ function with $\mathbf{V}$ from time level n to time level $n+1$,

Stage 3: replace the advected $\bar{\phi}^{n+1}$ by a reinitialised or redistanced $\tilde{\phi}^{n+1}$ in order to satisfy the condition:

$$meas(-\eta \leq \phi \leq \eta) \leq K_1\eta \tag{7}$$

time step after time step,

Stage 4: replace the re-initialised $\tilde{\phi}^{n+1}$ by a ϕ^{n+1} enjoying a conservation property,

Stage 5: compute a volumic extension of the zero contour curvature.

Stage 6: advance Equation (5) for moments .

This desserves some comments:
In stage 1, the advection velocity for the level set is not necessarily the material velocity. This point will be discussed in Section 4. Condition (7) in stage 3 controls the level set function gradient near the zero contour. In practice, function ϕ is re-initialised, i.e. replaced periodically by a function satisfying surely condition (7). In ([7],[8],[9])), a signed distance is built by solving to steady-state an Hamilton-Jacobi equation. In our study, the basic option is to rebuilt a distance from a geometrical algorithm, defining ϕ_{dist} at each vertex as the minimum distance to discrete zero countour of ϕ. For stage 4, we use a global volume conservation correction; a small perturbation C_ϕ is added to ϕ in each point of the domain to ensure conservation

$$\overline{\phi}_h^{n+1} \;=\; \phi_h^{n+1} + C_{\phi_h},\;\; \int H(\overline{\phi}_h^{n+1})dv = \int H(\phi_h^n)dv$$

As far as $H(\phi_h)$ is an higher order accurate approximation of χ, the error in $\int |H(\phi_h) - \chi|dv$ is of higher order and the global volume correction step will not degrade the accuracy.

3 Error analysis of Level Set advection

The LS method has permitted a lot of accurate applications, particularly in combination with cartesian meshes. Taking into account irregular meshes is a more difficult task, since in general, approximation convergence applied to the unknown functions and not to their derivatives and boundary traces. Fortunately, assuming only a L^p $(p \geq 1)$ convergence of the level set, we can still get an interesting approximation error estimate. Let us assume that we know how to numerically advect the level set ϕ by approximating it with a discrete level set function ϕ_h. Since ϕ is advected, the usual convergence property for ϕ_h on non-regular meshes is a convergence in L^p,

possibly of high-order. Let us examine the consequence for the corresponding $\chi_\phi = H(\phi)$ functions.

Proposition 1: *Let ϕ be a $L^p(Q)$ function where $Q = \Omega\times]0,T[$ is the flow integration domain in space and time. Let $(\phi_h)_h$ a sequence of $L^p(Q)$ we assume that:*

$$meas(-\eta \leq \phi \leq \eta) \leq K_1\eta \tag{8}$$
$$\| \phi_h - \phi \|_{L^p(Q)} \leq K_2 h^k \tag{9}$$

with h,η sufficiently small, k the convergence order on ϕ and K_1,K_2 independant of h,η then for all real number $q \geq 1$, there is a constant $C(q)$ independant of h such as

$$\| H(\phi_h) - H(\phi) \|_{L^q(Q)} \leq C(q) h^{\frac{2k}{3q}}. \tag{10}$$

Proof: the above integral can be decomposed as follows:

$$\begin{aligned}\int_Q |H(\phi_h) - H(\phi)| d\Omega dt &\leq meas(|\phi| \leq \eta) + meas(|\phi_h| \leq \eta) \\ &\quad + meas(\phi \geq \eta, \phi_h \leq -\eta) + meas(\phi \leq -\eta, \phi_h \geq \eta) \\ &\leq meas(|\phi| \leq \eta) + meas(|\phi_h| \leq \eta) + meas(|\phi_h - \phi| \geq 2\eta)\end{aligned}$$

but

$$meas(|\phi| \leq \eta) \leq K_1\eta, \text{ according to (8)}$$

and

$$\begin{aligned}meas(|\phi_h| \leq \eta) &\leq meas(|\phi| \leq 2\eta) \\ &+ meas(|\phi_h - \phi| \geq \eta),\end{aligned}$$

that is

$$meas(|\phi_h| \leq \eta) \leq 2K_1\eta + meas(|\phi_h - \phi| \geq \eta)$$

thus

$$\int_Q |H(\phi_h) - H(\phi)| d\Omega dt \leq 3K_1\eta + 2meas(|\phi_h - \phi| \geq \eta)\ . \tag{11}$$

The last sum part can be estimated as follows:

$$meas(|\phi_h - \phi| \geq \eta) = \int_{|\phi_h - \phi|^p \geq \eta^p} 1\ d\Omega dt \leq \frac{1}{\eta^p} \int_{|\phi_h - \phi|^p \geq \eta^p} |\phi_h - \phi|^p d\Omega dt \leq \frac{1}{\eta^p} ||\phi_h - \phi||^p_{L^p(Q)} \tag{12}$$

and with (11) and (12), we get:

$$\int_Q |H(\phi_h) - H(\phi)| d\Omega dt \leq 3K_1\eta + \frac{2}{\eta^p} ||\phi_h - \phi||^p_{L^p(Q)}\ .$$

By choosing $\eta = h^\theta$, $\theta = \frac{pk}{p+1}$, we get

$$\int_Q |H(\phi_h) - H(\phi)| d\Omega dt \leq 3K_1 h^\theta + 2K_2^2 h^{-p\theta} h^{pk} \leq (3K_1 + 2K_2^2) h^{\frac{pk}{p+1}},$$

thus

$$\int_Q |H(\phi_h) - H(\phi)| d\Omega dt \leq (3K_1 + 2K_2^2) h^{\frac{pk}{p+1}}$$

or equivalently, for $q \geq 1$:

$$||H(\phi_h) - H(\phi)||_{L^q} \leq K_5 h^{\frac{pk}{q(p+1)}}\ .\square \tag{13}$$

Remark 1: Assumption on convergence of $||\phi_h - \phi||_{L^p}$ is inspired by the L^2 convergence which can be obtained by an unstructured, P_1-continuous finite-element approximation for the advection of ϕ. □

Remark 2: Estimate (13) is not optimal and the order of accuracy is located between $\frac{pk}{q(p+1)}$ and k. In the sequel we shall refer to the case $p = 2, q = 1$, which give an order between $\frac{2k}{3}$ and k. □

The above analysis suggest that in order to get a global second-order convergence for a level set multifluid calculation, a second-order Navier-Stokes approximation should be combined with a **third-order** accurate advection of functions ϕ. This is the option taken in the sequel.

4 Interface variables extension

The LS method relies on the representation of several variables defined on the interface as volumic variables:
- the interface location is extended into a LS function,
- the interface velocity is used under a volumic shape,
- for capillarity, the interface normal and curvature also become volumic fields.

We observe that there is some constraints on these representations. They must be smooth enough, easy to compute accurately. Lastly, Condition (7) on LS gradient is a rather constraining one. However, these conditions still allow for many possible choices between the possible extensions of the above variables. The purpose of the reinitialisation Stage 3 is to replace function ϕ by a new one of same zero contour but satisfying Condition (7). Further, this new function should be smooth enough to permit an accurate computation of interface curvature. In the discrete case, there is no guarantee that the new function has exactly the same zero contour, nor that it will be enough smooth. If the advection step provides a ϕ function which already satisfies, at least close to interface, the unit gradient condition. we can imagine that error in reinitialisation step can be made smaller, because the reinitialisation step needs not large changes of function ϕ or even needs not changing it at all. In order to improve these points, we propose to reconsider **either interface motion direction**, **or the extension of level set function from interface**, which concerns Stage 3 (both option can also be combined).

4.1 Parametrizing LS extensions

LS function's gradient has to be controlled in order to satisfy condition (7). In usual LS method, this is performed by two means: (1) a canonical extension of the zero level is built with a signed distance, and (2) LS function is advected with the material velocity $\mathbf{U}$. To build a more general context, we identify two design criteria:
- control of LS gradient,
- consistent interface motion,

and we consider two main choices:
- the canonic LS extension.
- the interface velocity,

We restrict to 2D case for simplicity.

Consistent interface motion: let us return to the advection of the characteristic function χ which writes (in sense of distributions):

$$\frac{\partial \chi}{\partial t} \; + \; \mathbf{U}\cdot\nabla \, \chi \; = \; 0 \quad (\chi = 0 \; or \; 1) \; . \tag{14}$$

Let $\mathbf{n}_\chi$ be the normal vector to the interface Γ and τ_χ the tangential vector to the interface, i.e. such as $\nabla\chi\cdot\tau_\chi \; = \; 0$. The function χ is equivalently advected with any velocity $\mathbf{V}'$ such that:

$$(\mathbf{U} - \mathbf{V}^{'})\cdot\mathbf{n}_\chi \; = \; 0 \;\; \text{on} \;\; \Gamma \;\; , \;\; \forall \, t > 0 \; . \tag{15}$$

To parameterize the set of possible $\mathbf{V}'$ over the whole computational domain we first introduce a unit field specifying in the whole domain the direction of motion. Let $\widetilde{\mathbf{V}}_\Gamma$ be a vector defined on Ω such that

$$\widetilde{\mathbf{V}}_\Gamma \cdot \mathbf{n}_\chi \neq 0$$
$$|\widetilde{\mathbf{V}}_\Gamma| = 1.$$

If we construct a scalar field α such that

$$\alpha \;=\; \frac{<\mathbf{V}, \mathbf{n}_\chi>}{<\widetilde{\mathbf{V}}_\Gamma, \mathbf{n}_\chi>} \quad \text{on the interface}$$

then the vector field $\mathbf{V}' \;=\; \alpha\widetilde{\mathbf{V}}_\Gamma$ advects χ in an equivalent way to $\mathbf{U}$. To complete the definition of $\mathbf{V}'$, it remains to define an extension of α

LS gradient control: we look for an advection step which conserves in a neighborhood of interface LS function's streamline derivative, i.e. ϕ's derivative parallel to interface velocity. Interface velocity gradient needs be zero in this neighborhood. We need a streamline constant extension operator for this velocity:

Constant extension: $\alpha \mapsto \widetilde{S}\alpha$: given α on the interface, we can extend it along the field $\widetilde{\mathbf{V}}_\Gamma$ by imposing its extension $\widetilde{S}\alpha$ to be constant on each trajectory. This extends the interface velocity $\mathbf{V}'$:

$$\widetilde{\mathbf{V}}_\Gamma.\nabla\widetilde{S}\alpha \;=\; 0 \tag{16}$$
$$\mathbf{V}' \;=\; \widetilde{S}\alpha\widetilde{\mathbf{V}}_\Gamma \;. \tag{17}$$

In a dual manner, the corresponding extension operator for ϕ is a constant-gradient extension operator:

Constant-gradient extension: $\phi \mapsto \widetilde{P}\phi$: given a scalar field ϕ on the interface, we can define $\widetilde{P}\phi$ as the function equal to ϕ on the interface and such that:

$$\widetilde{\mathbf{V}}_\Gamma.\nabla\widetilde{P}\phi \;=\; 1 \;. \tag{18}$$

The main properties of our construction is now summed up:

Proposition 2: *Starting from a LS function satisfying the gradient property (18), for example defined as* $\widetilde{P}\phi$ *, and advecting it with the streamline constant extension* $\mathbf{V}' = \widetilde{S}\alpha\widetilde{\mathbf{V}}_\Gamma$

$$\frac{\partial\widetilde{P}\phi}{\partial t} \;+\; \widetilde{S}\alpha\widetilde{\mathbf{V}}_\Gamma\cdot\nabla\widetilde{P}\phi \;=\; 0 \;. \tag{19}$$

will produce an advected ϕ *which still satisfies the gradient property (18) in the vicinity of interface.*

Proof: We assume that we can construct a prolongation of ϕ such that

$$\nabla\widetilde{P}\phi \cdot \widetilde{\mathbf{V}}_\Gamma = 1 \text{ with } \widetilde{\mathbf{V}}_\Gamma \text{ constant in time}$$

To demonstrate that $\nabla\widetilde{P}\phi \cdot \widetilde{\mathbf{V}}_\Gamma$ is constant in time, we use (16),(18) and (19):

$$\frac{\delta(\nabla\widetilde{P}\phi \cdot \widetilde{\mathbf{V}}_\Gamma)}{\delta t} = \frac{\nabla\widetilde{P}\phi}{\delta t} \cdot \widetilde{\mathbf{V}}_\Gamma = \nabla(\frac{\widetilde{P}\phi}{\delta t}) \cdot \widetilde{\mathbf{V}}_\Gamma = -\nabla(\widetilde{S}\alpha\widetilde{\mathbf{V}} \cdot \nabla\widetilde{P}\phi) \cdot \widetilde{\mathbf{V}}_\Gamma = -\nabla\widetilde{S}\alpha \cdot \widetilde{\mathbf{V}}_\Gamma = 0.\square$$

4.2 A dilemma

The important consequence of Proposition 4 is that since (18) is satisfied, the reinitialization will not introduce a large error or can in some case be purely skipped. However, the operation of taking the trace of the velocity $\mathbf{V}$ on the interface Γ introduce a new error which needs to be analysed. We assume that :
- either the velocity is a smooth known function $\mathbf{V}$ which we interpolate on P_1 functions. $\mathbf{V}_h = \Pi_h \mathbf{V}$. then for $s = 0$ and 1:

$$||\mathbf{V}_h - \mathbf{V}||_{H^s} = ||\Pi_h \mathbf{V} - \mathbf{V}||_{H^s} \leq K(\mathbf{V}) h^{2-s} , \tag{20}$$

- or the velocity is accurately computed from a discretized system satisfying the following error estimate:

$$||\mathbf{V}_h - \mathbf{V}||_{H^s} \leq K(\mathbf{V}) h^{2-s} . \tag{21}$$

By the trace theorem and by the convexity inequality, we get:

$$||\mathbf{V} - \mathbf{V}_h||_{L^2(\Gamma)} \leq K_1(\mathbf{V}) \, ||\mathbf{V} - \mathbf{V}_h||_{H^{\frac{1}{2}}} \leq K_2(\mathbf{V}) \, ||\mathbf{V} - \mathbf{V}_h||_{H^0}^{\frac{1}{2}} ||\mathbf{V} - \mathbf{V}_h||_{H^1}^{\frac{1}{2}} \leq K_3(\mathbf{V}) \, h^{\frac{3}{2}} \tag{22}$$

This means that working with any extension of the velocity from its trace on the interface implies a lost of accuracy order with a gap of $\frac{1}{2}$, in particular:

Proposition 3: *With a second-order accurate Navier-Stokes scheme, we can expect an accuracy order of at least* $\frac{3}{2}$.

To sum up, it is possible to build a velocity field which avoids to some degree the error associated to redistancing but some other loss of accuracy may arise, especially when irregular/unstructured meshes are used, due to the fact that we take a trace of advection velocity on the interface.

4.3 Provisional conclusion

We have identified a general class of interface velocity and extension. The impact on global accuracy is analysed. In the absence of wall effect, re-initialisation by a signed distance can be improved by increasing the consistency of the combined advection and redistancing steps. When the problem under study involves a contact angle condition, we shall choose in Sec.6 a different re-initialisation.

5 First experiment: capillary instability

This section is devoted to illustrate Sec.3. We investigate how accurate is the level set algorithm based on a reinitialisation by signed distance and the third-order advection scheme of the LS function. We consider the Rayleigh instability of a liquid cylinder in the case where capillary effects are dominant. The cylinder is perturbed with a perturbation equation in the half plane ($x > 0$) containing the symmetry axis of the cylinder defined as

$$x = a + \eta \, sin(\frac{2\pi y}{\lambda_d} + K_1) \tag{23}$$

in which λ_d and η are respectively the wave length and the perturbation height. For $\lambda_d > 2\pi a$ where a is the liquid cylinder radius, the perturbation amplifies.
We use the numerical algorithm, stages 1 to stage 6, described in the second section, with:
- an axisymmetric formulation,
- for advecting the LS function, we use a third-order accurate upwind-biased scheme which enjoys third-order accuracy on regular meshes,
- a geometric re-distancing of ϕ every ten time steps,
- a mass conservation of each disconnected phase in the manner described at the end of the third section,
- a second-order accurate vertex-centered mixed finite-element/finite-volume method with projection for advancing the velocity.

Surface tension Coefficient	:	$\sigma = 0.07275\ SI$
Liquid cylinder radius	:	$r = 0.01\ m$
Density ratio	:	$\rho_l = 1000\ kg.m^3\ \rho_g = 1.2\ kg.m^3$
Computation domain size	:	$L_x = 0.01\ m\ L_y = 0.02\ m$
$a = 0.0025\ m\ \lambda_d = 0.02\ m$		

Table 1: Test case: Capillary instability

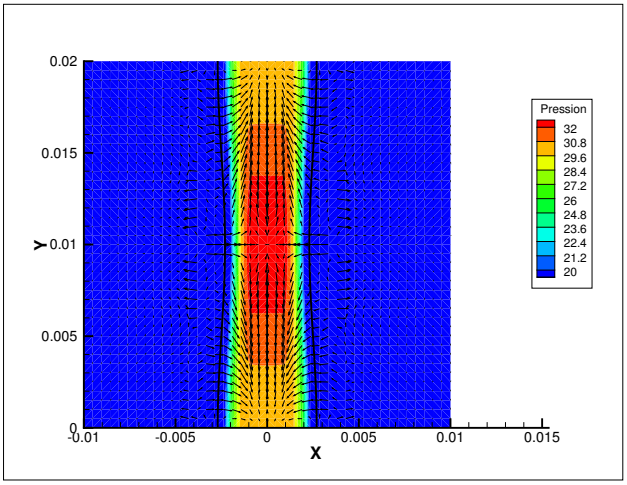

Figure 1: *Initialisation of the perturbation. Vizualisation of pressure field, velocity vectors and interface (black line).*

According to the previous analysis, a global second-order spatial accuracy should hold for regular cases.

We measure the numerical order of accuracy before and after the formation of a drop. The different parameters of the test case are described in Tab.1. We compare the results obtained with three meshes embedded with respectively 902, 3402 and 13202 mesh nodes (grid space step respectively of $4h$, $2h$ and h with $h = 0.125\ mm$).

The breaking occurs at $t = 0.136\ s$ for the coarse mesh, $t = 0.125\ s$ for the intermediate mesh and $t = 0.122\ s$ for the fine mesh. We measure the convergence on both the L_2 error norm of ϕ and the L_1 error norm of $H(\phi)$ at $t = 0.11\ s$ (before the breaking for the three meshes) $t = 0.12\ s$, and $t = 0.13\ s$ (after the breaking for all meshes). Fig.2 and 3 representing the mesh convergence on interface location at $t = 0.11\ s$,$t = 0.12s\ s$ and $t = 0.13\ s$ give already a visual idea of the accuracy lost. Tab. 2 shows the convergence order on the deviations

$$||\phi_h - \phi_{2h}||_{L_2} \text{ and } ||H(\phi_h) - H(\phi_{2h})||_{L_1}$$

between embedded meshes. The numerical convergence order is evaluated through computations on three embedded meshes by the following equation

$$n = \frac{log(\frac{||\Psi_{2h} - \Psi_{4h}||}{||\Psi_h - \Psi_{2h}||})}{log(2)}, \tag{24}$$

where Ψ_h,Ψ_{2h} and Ψ_{4h} are discrete solutions on the mesh with h,$2h$ and $4h$ as space step.
Beginning of Tab. 2 and Fig.2 illustrate the case for which our error analysis of the third section applies. Tab. 2 shows a numerical order of convergence on $||H(\phi_h)||_{L_1}$ even better than L_2 error on ϕ. Considering that we use a third-order accurate scheme for the advection of ϕ, this result shows a better order than predicted by the lower estimate of Section 3. At time $t = 0.13$, breaking occured for medium and fine meshes but not for the coarse-mesh computation. The accuracy on that coarse mesh is much degraded for the ϕ function. The level of error for $H(\phi)$ becomes also

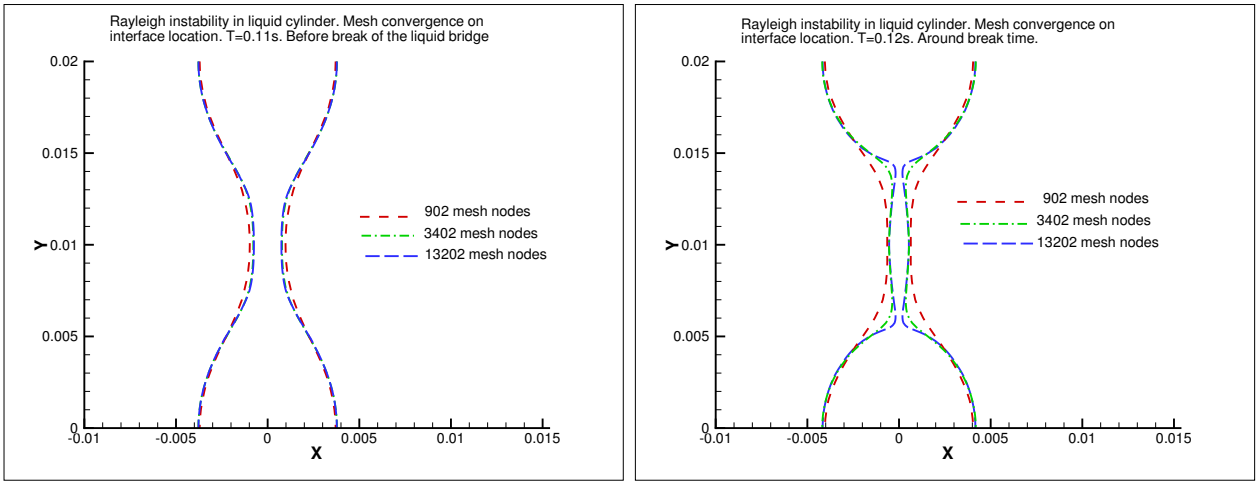

Figure 2: *Left: Mesh convergence on interface at T=0.11s Right: Mesh convergence on interface at T=0.12s.*

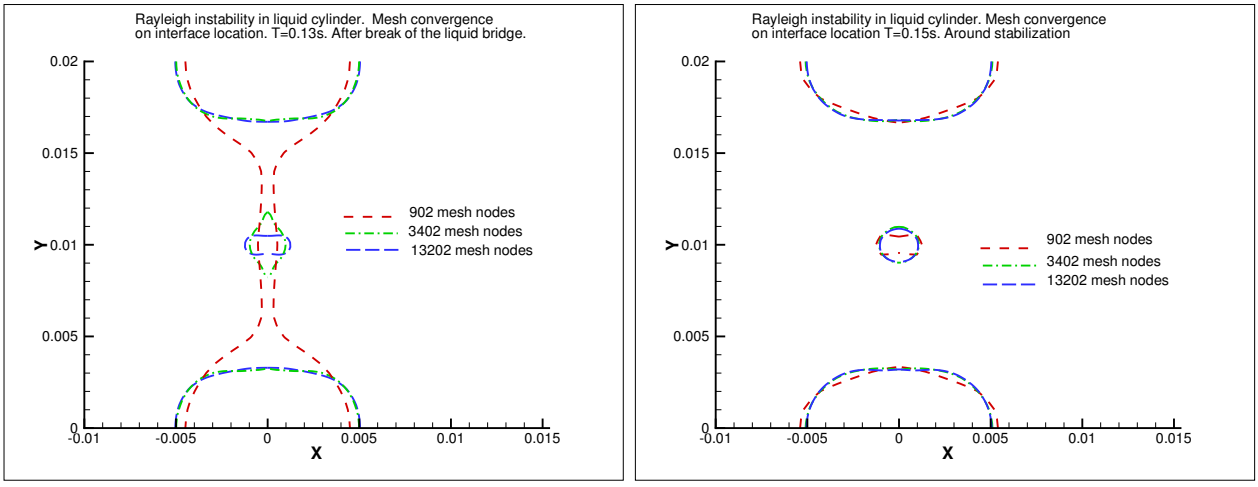

Figure 3: *Left: Mesh convergence on interface at T=0.13s. Right: Mesh convergence on interface at T=0.15s.*

Physical time (s.)	Grid size	L_2 deviation on ϕ	L_1 deviation on $H(\phi)$
0.11	902	-	-
0.11	3402	$1.6253.10^{-6}$	$2.45461.10^{-6}$
0.11	13202	$2.46967.10^{-7}$	$3.23397.10^{-7}$
0.11	Numerical order	2.7	2.92
0.12	902	-	-
0.12	3402	$2.982.10^{-6}$	$5.515.10^{-6}$
0.12	13202	$7.915.10^{-7}$	$1.520.10^{-6}$
0.12	Numerical order	1.91	1.86
0.13	902	-	-
0.13	3402	$9.33789.10^{-6}$	$1.38947.10^{-5}$
0.13	13202	$3.233.10^{-6}$	$2.236.10^{-6}$
0.13	Numerical order	1.53	2.63

Table 2: Capillary instability. Numerical order on the interface position at $t = 0.11s$, $t = 0.12s$, and $t = 0.13s$.

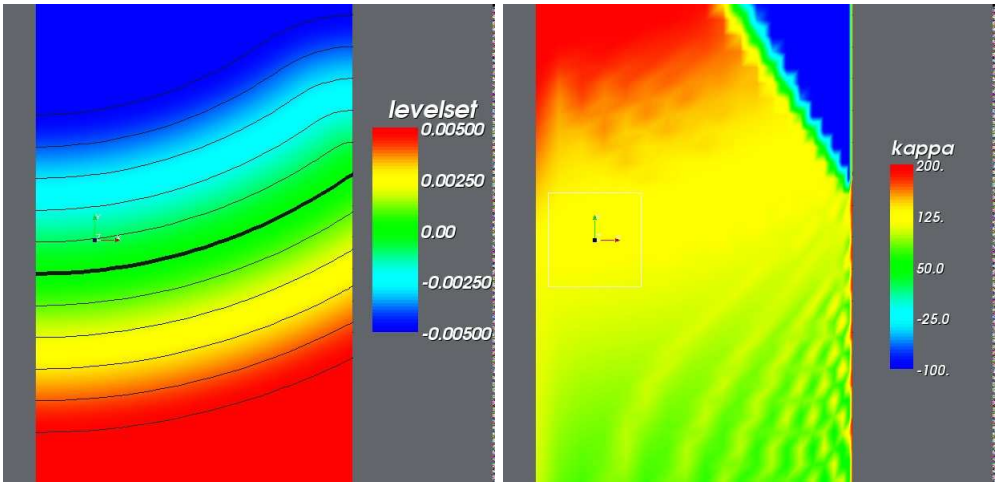

Figure 4: *Equilibrium circular meniscus with contact angle. Left: Signed Distance ϕ function . Thickened line represents the interface. Right: Curvature "κ" computed as 2^{nd} derivative of ϕ.*

high for the coarse mesh and the high numerical order measured is not significative of anything but the large error of coarse mesh.

6 Application to capillarity with contact angle

We consider now the numerical modelling of axisymmetric capillary effects with gravity and contact angle in a vertical tube. In the differential model that we study, a prescribed static angle β_S is satisfied by the interface. In terms of the level set function, this means that at contact point A we have:

$$\nabla\phi(A).\mathbf{n}_\Sigma \;=\; cos(\beta_S)\ .$$

Since β_S is generally not equal to $\pi/2$, the corresponding signed distance to interface is not smooth in the vicinity of contact point. A consequence is that interface curvature is more difficult to evaluate from the level set function (6) as we can observe on Fig.4. We need consider another option for re-initialisation of ϕ. Then, excluding the particular case of a $\pi/2$ contact angle, we observe that the option consisting of advecting the interface with a normal-to-interface velocity

seems not well adapted to the contact point motion. In the next section in the case of a vertical wall, we propose an axial velocity field construction and an axial extension operator and we study their impact on the computation of the reorientation of a free surface after a sudden decreasing of gravity to zero.

6.1 Axial velocity field and axial extension operator

With the particular geometry of a tube, we can use a very simple particular case of the previous theory. We take as velocity $\widetilde{\mathbf{V}}_\Gamma$ the constant unitary field parallel to vertical axis:

$$\widetilde{\mathbf{V}}_\Gamma = e_z$$

At an instant t, we extend the level set function from the interface position ($\phi_\Gamma = 0$) along e_z, with :

$$\frac{\delta\phi}{\delta z} \;=\; 1\ . \tag{25}$$

Let $h_p = f(r)$ be the bijective representation of the interface. We define function ϕ's z-affine extension with:

$$\phi(r,z) = -(z - h_p(r))\ . \tag{26}$$

As the represention of the interface can be represented as a bijective funtion $h_p = f(r)$ and the contact angle not equal to zero.
According to the above theory, for any point $M(r,z)$ of Γ, we have

$$e_z \cdot \mathbf{n}_\chi \;\neq\; 0\ .$$

We derive a new velocity field $\mathbf{V}^{'}$ as follows:

$$\mathbf{V}^{'} \;=\; \alpha e_z \quad \text{and} \quad \mathbf{V}^{'} = (\mathbf{U}\cdot\mathbf{n}_\chi)\cdot\mathbf{n}_\chi + \beta\tau_\chi.$$

This choice allows the satisfaction of Condition (7) specified in Section 2 as far as the interface orientation does not show vertical parts, i.e. its normal is never orthogonal to z-axis.

$$\mathbf{V}^{'}_r \;=\; 0 \;= ((\mathbf{U}\cdot n)\cdot n)_r + \beta\tau_r \tag{27}$$

$$\mathbf{V}^{'}_z \;=\; ((\mathbf{U}\cdot n)\cdot n)_z + \beta\tau_z \tag{28}$$

$$\beta = \frac{-((\mathbf{U}\cdot n)\cdot n)_r}{\tau_r} \tag{29}$$

$$\mathbf{V}^{'}_z \;=\; \alpha e_z \;\text{ with }\; \alpha \;= ((\mathbf{U}\cdot n)\cdot n)\cdot e_z + \beta\tau_z \tag{30}$$

In the whole domain $\mathbf{V}^{'}(r,z) = \alpha(r)e_z$ where $\alpha(r)$ is the value of α at radius r on Γ. Fig.5 shows the desired transformation. The advancing of ϕ in time with $\mathbf{V}^{'}(r,z)$ keeps the property $\phi(r,z) = -(z - h_p(r))$. On Fig.6, we can also observe how the extension of the ϕ fonction along e_z improves the computation of the curvature on a circular equilibrium interface compared to the case of ϕ as a signed distance to the interface.

6.2 Numerical results

We consider the reorientation computation of a free surface in an axisymmetric vertical cylinder after a sudden decreasing of the gravity to zero. The motion is dominated by two effects, the surface tension force and the contact angle at wall. In this study, we are interested by numerical accuracy and we restrict our study to a constant contact angle model.

The reoriented liquid (first phase) is M_3 with physical properties given in Tab. 3.
We refer to the works of ZARM research center of Bremen, ([11],[12],[13]) for further details and for investigations of physical aspects of the problem under study. The model is viscous, two-phase Navier-Stokes equations for an incompressible fluid, involving surface tension effects and a fixed

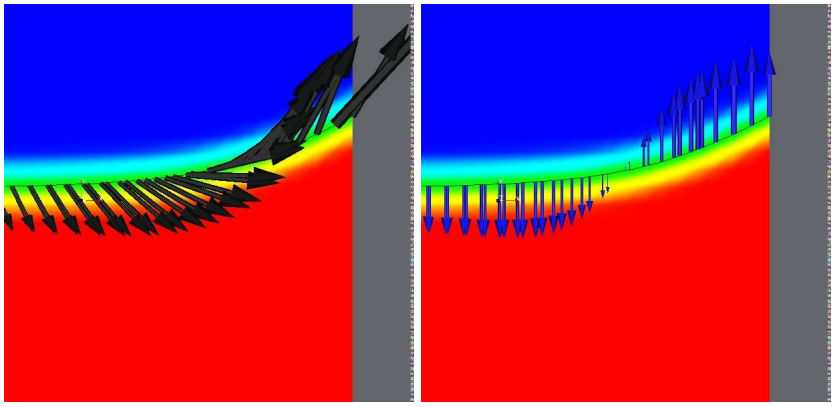

Figure 5: *Transformation of the velocity field* $\mathbf{V} \rightarrow \mathbf{V}' = \alpha\widetilde{\mathbf{V}}$ *with* $\widetilde{\mathbf{V}} = e_z$.

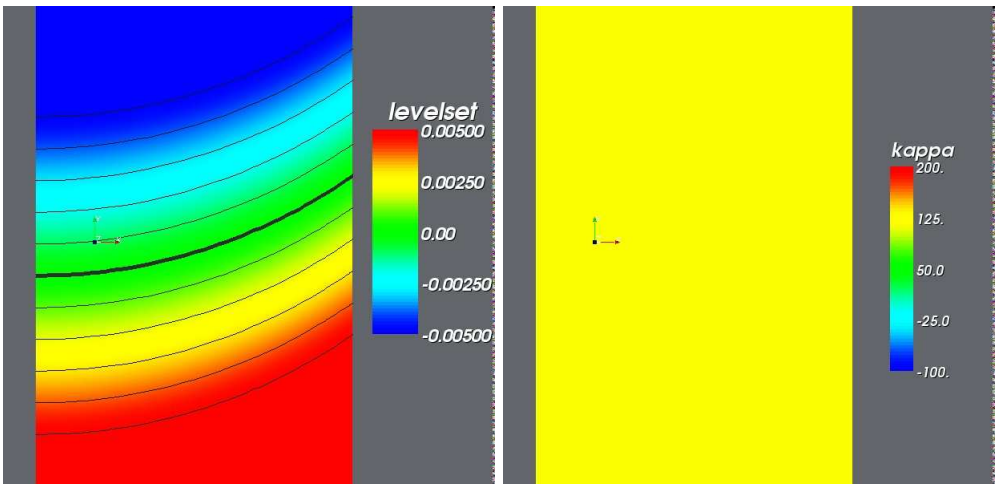

Figure 6: *Equilibrium circular meniscus with contact angle. Left:* ϕ *function extended along* e_z. *Right: Curvature "*κ*" computed as* 2^{nd} *derivative of* ϕ *extended along* e_z. *Thickened line represents the interface.*

Dynamic viscosity of the liquid	:	$2.566\ 10^{-3}\ kg.m^{-1}.s$
Contact angle	:	55 degrees
Surface tension coefficient	:	$\sigma\ =\ 0.0181074\ SI$
Cylinder radius	:	$r\ =\ 0.01\ m$
Cylinder height	:	$h\ =\ 0.048\ m$
Density values	:	$\rho_l\ =\ 879\ kg.m^3\ \rho_g\ =\ 1.2\ kg.m^3$

Table 3: Physical properties of liquid phase

Number of nodes in the cylinder radius	L_2 deviation norm on ϕ	L_1 deviation norm on $H(\phi)$
11	-	-
21	$1.06668.10^{-7}$	$3.40992.10^{-8}$
41	$5.32013.10^{-8}$	$1.45119.10^{-8}$
Numerical order	1.003	1.233
81	$2.51436.10^{-8}$	$4.73495.10^{-9}$
Numerical order	1.081	1.62

Table 4: Capillary meniscus reorientation. Numerical order on the deviation norms at $t = 0.005s$ for **Scheme 1.**

contact angle. The numerical scheme relies on a continuous linear finite element approximation for level set function, velocities and pressure, with a time-advancing combining an explicit advection diffusion and a pressure projection. The surface tension coupling is modelled with a thickened interface [10]. The contact angle β_S is maintained to 55 degrees. We compute the reorientation oscillations over $t = 4.7s$ on four meshes embedded but not uniform (refined on the wall) with respectively $11, 21, 41, 81$ grid nodes in the cylinder radius. The reorientation starts from a flat free surface with large curvature and contact angle on the wall, to oscillate around the final equilibrium free surface which is a spherical cap(constant curvature). Fig.7 shows the smooth advection of the interface other the first $0.05s$. In such smooth conditions,we can make a convergence study at $t = 0.005s$ $t = 0.01s$, $t = 0.02s$ for two schemes to get a confirmation of the two estimates (13) and (22). We initialize the level set function ϕ as the z-affine extension introduced in (26). We test two advection schemes for ϕ:
- **Scheme 1** we advect ϕ with the axial velocity field (30) deduced from the physical velocity and apply no reinitialisation.
- **Scheme 2** we advect ϕ with the physical velocity and we reinitialise the ϕ as the z-affine extension introduced in (26).

Fig.8 shows the mesh convergence on the time evolution of the interface position on the wall using **Scheme 2** for the computation. We measured a global second-order convergence on the contact point of interface location at the maxima of this curve ($t \approx 0.12s$). To measure the convergence on global interface position, we consider the same norms as before, i.e. $||\phi_h - \phi_{2h}||_{L_2}$ and $H(\phi)$, $||H(\phi_h) - H(\phi_{2h})||_{L_1}$. Tabs.4 and 5 show lower numerical convergence. Tab.4 shows however a less good convergence of the deviation norm L_2 on ϕ for **Scheme 1** than for **Scheme 2**. This numerical result confirmed our estimation done on the trace (22). However, in our variational implementation of curvature at contact angle a singularity remains during the transient phases. It is probably the main obstacle to full second-order accuracy.

Number of nodes in the cylinder radius	L_2 deviation norm on ϕ	L_1 deviation norm on $H(\phi)$
11	-	-
21	$1.10242.10^{-7}$	$3.43735.10^{-8}$
41	$4.72528.10^{-8}$	$1.38395.10^{-8}$
Numerical order	1.22	1.31
81	$1.84879.10^{-8}$	$4.70746.10^{-9}$
Numerical order	1.35	1.555

Table 5: Capillary meniscus reorientation. Numerical order on the deviation norms at $t = 0.005s$ for **Scheme 2.**

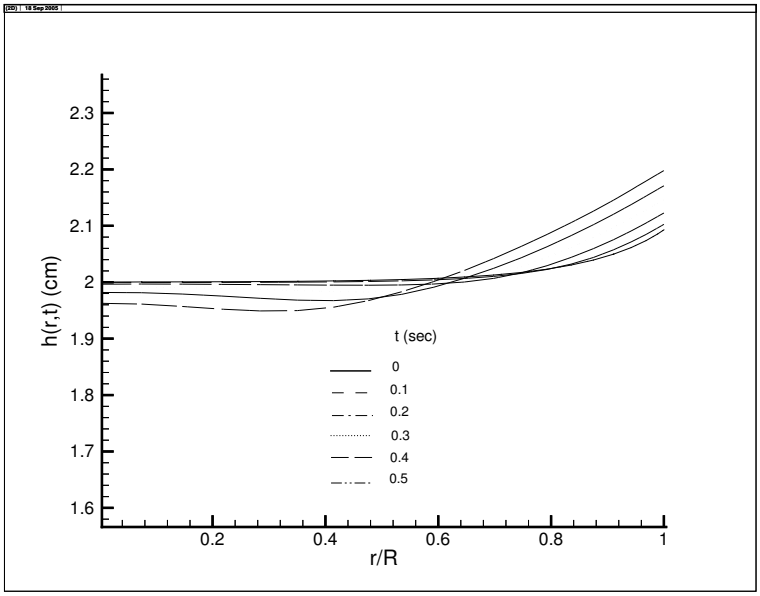

Figure 7: *Capillary reorientation. Free surface evolution* $t = 0.; 0.01; 0.02; 0.03; 0.04; 0.05s$.

7 Concluding remarks

The level set principle introduces a smooth function ϕ in place of a step function, opening the door to higher-order accuracy advection. However, dependant variable ϕ has to be re-initialised periodically, in a way that introduce as small new errors as possible. We analyse with only very few assumptions how higher order can be obtained, and under which conditions. We then define a large set of possible interface velocities constructions and of possible level set re-initialisations and we study the interaction between these options.

The first part of the analysis is confronted with the practical calculation of a capillary Rayleigh instability. In this flow, although a singularity appears at breaking time, the overall accuracy remains close to second order.

In the case of a capillarity phenomena with contact angle, we propose to avoid as much as possible any non-physical singularity. The proposed extension of level set function provides a smooth curvature field and is of paramount impact on global accuracy. The proposed extension of interface velocity proves to perform rather well, but not better than advecting level set directly with material velocity field.

In a general geometry, an extension of the proposed method would involve the evaluation of the parameterizing field by a numerical algorithm. Under this condition, the method would extend to 3D geometries.

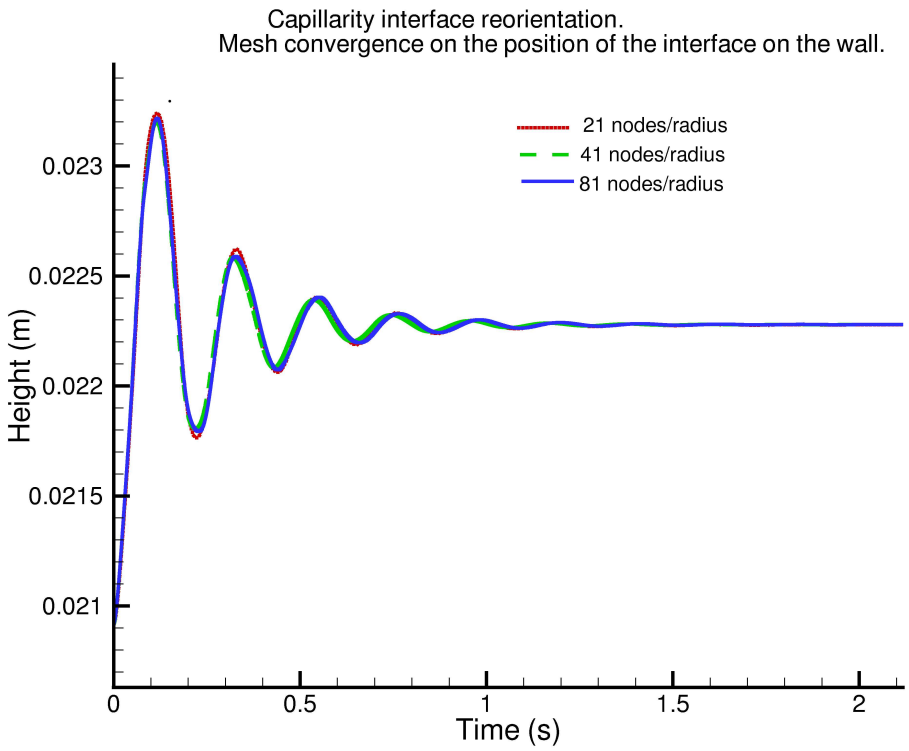

Figure 8: *Capillary reorientation. Mesh convergence for the interface position on the wall.*

8 Acknowledgments

The first author was partly supported by a scientific scholarship of Région Provence-Alpes Côte d'Azur.

References

[1] J.E. Pilliod Jr and E.G. Puckett, "Second-order accurate volume-of-fluid Algorithms for tracking material interfaces", *J. Comput. Phys.* **199**(2), 465-502, 2004

[2] J. Simon, "Non-homogeneous viscous incompressible fluids: Existence of velocity, density and pressure". *SIAM J.Math.Anal.*, **21**(5), 1990.

[3] A.V. Kajikov and SA. Antonzev. "Mathematical Study of flows of non-homogeneous fluids". *Lectures at the University of Novosibirsk*, U.S.S.R., 1973. (In Russian).

[4] C.W. Hirt and B.D. Nichols, "Volume of Fluid (VOF) methods for the dynamics of free boundaries", *J. Comput. Phys.* **30**, 201-255, 1981.

[5] J. Brackbill, D.B. Kothe and C. Zemach, "A continuum method for modeling surface tension", *J. Comput. Phys.* **100**, 335-354, 1992.

[6] S. Osher and J.A Sethian, "Front propagating with curvature dependant speed: Algorithms based on Hamilto-Jacobi formulations", *J. Comput. Phys.* **79**(12), 1988.

[7] J.A. Sethian, "*Level Set Methods and Fast Marching Methods*" . Cambridge University Press, 1999.

[8] S. Osher and R. Fedkiw. "*Level Set Methods and Dynamic Implicit Surfaces*". Springer, 2002.

[9] M. Sussman, E. Fatemi, P. Smereka and S. Osher. "An improved level set method for incompressible two-phase flows." *Computers and Fluids*, **27**(5-6), pp. 663-680 (1998)).

[10] M. Sussman, P. Smereka and S. Osher. "An level set approach for computing solutions to incompressible two-phase flow", *J. Comput. Phys.* **114**, 146-159 (1994)).

[11] M. Dreyer and U. Schmid. "Testcase 3: Reorientation of a Liquid Surface after a Step Reduction of the Gravity." *In: experimental results of the COMPERE TEST CASES 1,2 and 3.* November 2000.

[12] G. Woelk, M. Dreyer, and H.J. Rath. "Damped oscillations of a liquid/gas surface upon step reduction in gravity".*Journal of Spacecraft and Rockets* **34**(1), 1997.

[13] S. van Mourik. "Numerical Modelling of the dynamic contact angle". *Master's Thesis.* University of Groeningen. Department of Mathematics (2002).